Galaxy evolution within the Kilo-Degree Survey

C. Tortora, N. R. Napolitano, F. La Barbera, N. Roy, M. Radovich, F. Getman,
M. Brescia, S. Cavuoti, M. Capaccioli, G. Longo and the KiDS collaboration

Abstract The ESO Public Kilo-Degree Survey (KiDS) is an optical wide-field imaging survey carried out with the VLT Survey Telescope and the OmegaCAM camera. KiDS will scan 1500 square degrees in four optical filters (u, g, r, i). Designed to be a weak lensing survey, it is ideal for galaxy evolution studies, thanks to the high spatial resolution of VST, the good seeing and the photometric depth. The surface photometry have provided with structural parameters (e.g. size and Sérsic index), aperture and total magnitudes have been used to derive photometric redshifts from Machine learning methods and stellar masses/luminositites from stellar population synthesis. Our project aimed at investigating the evolution of the colour and structural properties of galaxies with mass and environment up to redshift $z \sim 0.5$ and more, to put constraints on galaxy evolution processes, as galaxy mergers.

We start from the KiDS-Data Release 2 (DR2) multi-band source catalogs, based on source detection in the r-band images. Star/galaxy separation is based on the CLASS_STAR (star classification) and S/N (signal-to- noise ratio) parameters provided by S-Extractor [2, 12]. S-Extractor will provide with aperture photometry and Kron-like magnitude MAG_AUTO. From the original catalog of ~ 22 millions of sources, the star/galaxy separation leaves with a sample of ~ 7 millions of galaxies. To perform galaxy evolution studies and determine reliable structural parameters, the highest-quality sources have to be taken [12, 11]. Thus, we have fi-

C. Tortora e-mail: ctortora@na.astro.it, N.R. Napolitano, F. La Barbera, F. Getman, M. Brescia, S. Cavuoti

INAF – Osservatorio Astronomico di Capodimonte, Salita Moiariello, 16, 80131 - Napoli, Italy,

M. Radovich
NAF - Osservatorio Astronomico di Padova, vicolo dellOsservatorio 5, I-35122 Padova, Italy

N. Roy, M. Capaccioli, G. Longo
Department of Physics, University of Napoli Federico II, via Cinthia 9, 80126 Napoli, Italy

KiDS collaboration: http://kids.strw.leidenuniv.nl/team.php

nally selected those systems with the highest r-band signal-to-noise ratio (S/N), $S/N \equiv 1/\texttt{MAGERR\_AUTO\_r} > 50$, where $\texttt{MAGERR\_AUTO\_r}$ is the uncertainty of $\texttt{MAG\_AUTO}$. This sample will consist of ~ 380000 galaxies. In addition to aperture photometry and Kron-like magnitudes, the relevant data for each galaxy are listed in the following.

Fig. 1 2D fit output for an example galaxy from 2DPHOT. The top panels show the galaxy image (left) and the residual after the fit (right), while the six bottom panels provide residuals after subtraction, plotted as a function of the distance to the galaxy center, with each panel corresponding to a different bin of the polar angle. Residuals are normalized with the noise expected from the model in each pixel.
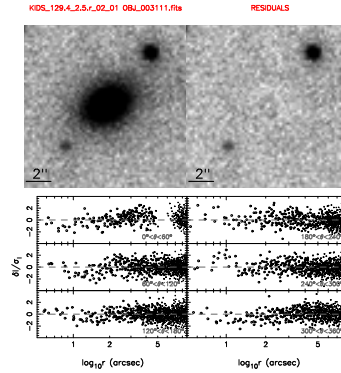
Structural parameters. Surface photometry is performed using the 2DPHOT environment. For each galaxy, a local PSF model is constructed by fitting the four closest stars to that galaxy. Galaxy images were fitted with PSF-convolved Sérsic models having elliptical isophotes plus a local background value [12]. The fit provides the following parameters: surface brightness μ_e, effective radius, R_e, Sérsic index, n, total magnitude, m_S, axis ratio, q, etc. Fig. 1 shows the 2DPHOT output for an example galaxy. For further details, see the contribution from Roy et al.

Photometric redshifts. Photo-z's are derived from KiDS ugri photometry using a supervised machine learning model, the Multi Layer Perceptron with Quasi Newton Algorithm (MLPQNA, [3]) within the DAMEWARE (DAta Mining and Exploration Web Application REsource, [4]). Supervised methods use a knowledge base (in our case with spectroscopic redshifts) of objects for which the output (in our case the redshift) is known a-priori to learn the mapping function that transforms the input data (our optical magnitudes) into the desired output (i.e. the photometric redshift). For this reason, our sample is cross-matched with spectroscopic samples from SDSS [1] and GAMA [8] surveys, which provide a redshift coverage up to $z \sim 0.8$. The knowledge base consists of ~ 60000 objects. 60% of these objects are used as train sample, and the remaining ones for the blind test set. The redshifts in the blind test sample resemble the spectroscopic redshifts quite well, with a scatter in the quantity $|z_{\mathrm{spec}} - z_{\mathrm{phot}}|/(1 + z_{\mathrm{spec}})$ of ~ 0.03. This approach reaches high accuracies with optical band only, and is far better than traditional spectral energy distribution (SED)-fitting methods. After these experiments the final catalogue of redshifts for our high-S/N sample is produced. See Cavuoti et al. (2015, in prep.) for details.

Rest-frame luminosities and stellar masses. Luminosities and stellar masses are made using the software $\texttt{Le Phare}$ [9], which performs a simple χ^2 fitting method between the stellar population synthesis (SPS) theoretical models and data. Models

from Bruzual & Charlot [5] and with a Chabrier IMF [6] are used. We adopt the observed ugri magnitudes (and related 1σ uncertainties) within a $3''$ aperture, which are corrected for Galactic extinction. Total Sérsic magnitudes, m_S, are used to correct the outcomes of `Le Phare` for missing flux.
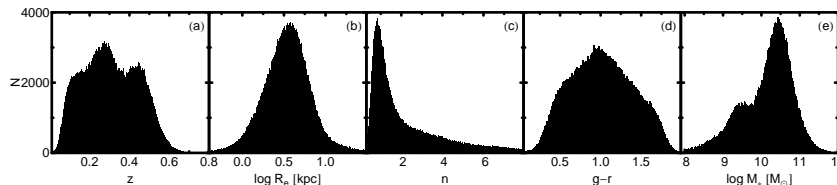

Fig. 2 Distribution of some galaxy parameters: photo-z, z (panel a), r-band effective radius $\log R_e/$kpc (panel b), r-band Sérsic index, n (panel c), observer-frame g-r colour within an aperture of $3''$ of radius (panel d) and Chabrier IMF-based stellar mass $\log M_\star/M_\odot$ (panel e).

This high-S/N sample is 90% complete down to a magnitude of `MAG_AUTO_r` ~ 21, which means that the sample is complete at masses $\gtrsim 5 \times 10^{10}$ up to redshift $z = 0.5$ (see Napolitano et al. 2015, in prep., for further details). The distribution of galaxy parameters for galaxies brighter than the completeness limit are shown in Fig. 2. The average redshift of the sample is $z = 0.3$, and the distribution reach the maximum redshifts of $z = 0.7$ (panel a). The distribution of effective radii is centered on ~ 3.5 kpc average value (panel b), while the average Sérsic index is ~ 1.5, but the distribution present a peak at $n \sim 0.8$, with a long tail to higher values (> 10, panel c). Thus, our datasample is dominated by late-type systems, which are characterized by low Sérsic indices [10, 16]. In the panel (d) we show the distribution of the observer-frame g-r colour, which have a median value of $g - r = 1$ and a symmetric distribution. These colours, when converted to rest-frame values, confirm the considerations made looking at the distribution of Sérsic index, since the median rest-frame colour is ~ 0.5, which is typical of a late-type blue galaxy. Finally, in panel (e) we plot the stellar mass distribution from SPS fitting, which presents a double-peaked distribution, with maxima at $\sim 2.5 \times 10^9$ and $\sim 2.5 \times 10^{10} M_\odot$, the median mass of the sample is $1.9 \times 10^{10} M_\odot$.

Aims of the project. The present galaxy evolution project will aim to achieve different objectives: the analysis of the colour-magnitude evolution, colour gradients, as the size and mass accretion in late- and early-type systems. By the end of the survey, we plan to collect about 3.5 millions of galaxies with high-quality photometry, i.e. *the largest sample of galaxies with measured structural parameters in the u, g, r and i bands, up to redshift $z = 0.7$.* KiDS will provide the bridge to connect the local environment to the high-redshift Universe, by means of this strong characterization of the internal structure of the galaxies. The study of the mass, colour and structural evolution of galaxies, connected with the outcomes of theoretical models and cosmological simulations provide a variegate set of information about the main physical processes which shape the galaxy evolution. In particular, taking benefit from the

good pixel scale and seeing, together with depth of VST telescope, we have scanned the first 156 sq. deg. of KiDS searching for massive ($M_\star > 8 \times 10^{10} M_\odot$) and compact ($R_e < 1.5$ kpc) galaxies, relic of massive galaxies at redshift $z = 2$ (see Tortora et al. 2015, in prep.). In some theoretical models the fraction of such massive and small objects, that could survive without having any significant transformation since $z \sim 2$, could reach a fraction about $1 - 10\%$ [13]. Previous observational works have not detected such old, compact and massive galaxies in the local universe [20]. In contrast, such peculiar objects are found at larger redshift [7]. A front-edge survey like KiDS will allow us to perform the census of these compact objects and trace their abundance and evolution in the last billions of years, contrasting the results with expectations from cosmological simulations. Finally, for a sample of KiDS galaxies with SDSS spectroscopy, we will perform the Jeans dynamical analysis of the measured velocity dispersions, to study dark matter fraction and Initial mass function in terms of redshift, mass, mass density and environment [17, 18, 19]. Testing the dependence of the Initial mass function by the mass density, using dynamics and spectral indices, can help to understand the results in Smith et al. [14], which find shallow IMF slopes in some high-velocity dispersion galaxies, in contrast with the current literature [17, 15].

References

1. Ahn C. P. et al., 2014, ApJS, 211, 17
2. Bertin E., Arnouts S., 1996, A&AS, 117, 393
3. Brescia M., Cavuoti S., Longo G., De Stefano V., 2014, A&A, 568, A126
4. Brescia M. et al., 2014, PASP, 126, 783
5. Bruzual G., Charlot S., 2003, MNRAS, 344, 1000
6. Chabrier G., 2001, ApJ, 554, 1274
7. Damjanov I., Hwang H. S., Geller M. J., Chilingarian I., 2014, ApJ, 793, 39
8. Driver S. P. et al., 2011, MNRAS, 413, 971
9. Ilbert O. et al., 2006, A&A, 457, 841
10. Kauffmann G. et al., 2003, MNRAS, 341, 54
11. La Barbera F. et al., 2010, MNRAS, 408, 1313
12. La Barbera F. et al., 2008, PASP, 120, 681
13. Quilis V., Trujillo I., 2013, ApJ, 773, L8
14. Smith, R. J., Lucey, J. R., & Conroy, C. 2015, MNRAS, 449, 3441
15. Spiniello, C., Barnabè, M., Koopmans, L. V. E., & Trager, S. C. 2015, arXiv:1505.07450
16. Tortora C. et al., 2010, MNRAS, 407, 144
17. Tortora C., Romanowsky A. J., Napolitano N. R., 2013, ApJ, 765, 8
18. Tortora C., La Barbera F., Napolitano N. R., Romanowsky A. J., Ferreras I., de Carvalho R. R., 2014, MNRAS, 445, 115
19. Tortora C., Napolitano N. R., Saglia R. P., Romanowsky A. J., Covone G., Capaccioli M., 2014, MNRAS, 445, 162
20. Trujillo I. et al., 2009, ApJ, 692, L118